IEEE Access
Multidisciplinary | Rapid Review | Open Access Journal

Received August 23, 2019, accepted September 11, 2019, date of publication September 18, 2019, date of current version October 2, 2019.

Digital Object Identifier 10.1109/ACCESS.2019.2942134

Source-Network-Storage Joint Planning Considering Energy Storage Systems and Wind Power Integration

XIAOSHENG WU AND YUEWEN JIANG
College of Electrical Engineering and Automation, Fuzhou University, Fuzhou 350108, China
Fujian Key Laboratory of New Energy Generation and Power Conversion, Fuzhou 350108, China

Corresponding author: Yuewen Jiang (jiangyuewen2008@163.com)

This work was supported in part by the Natural Science Foundation of China under Grant 51707040, and in part by the Natural Science Foundation of Fujian Province in China under Grant 2018J01482.

ABSTRACT With the large-scale grid integration of wind power, the inherent space-time characteristics of wind power and the transmission congestion seriously restrict the consumption of wind power and the development of demand. In order to improve the wind power accommodation and load acceptance level, the joint planning including the wind power installed capacity and location, the transmission network expansion, and energy storage system locating and sizing is considered. The generation-side operation process and the charging-discharging strategy of energy storage systems are also involved. The source-network-storage joint planning model is established with the goal of minimizing the cost of the transmission network expansion, the construction and operation of energy storage systems, the conventional units' operation, the wind curtailment, and the heavy-load penalty. Furthermore, the energy storage system planning & operation constraints, the heavy-load operation constraints and the quadratic generation cost function are linearized in the MILP model. Through the Wood&Wollenberg 6-bus system, the IEEE RTS-24 test system, and the modified IEEE 118-bus system as the test systems, the joint planning schemes under multiple scenarios are compared and analyzed. The results show that the proposed planning model can effectively improve the load acceptance capability and wind power integration level.

INDEX TERMS Energy storage system, linear programming, transmission grid expansion planning, unit commitment, wind power integration.

I. INTRODUCTION

With the increasing of demand and the proportion of renewable energy sources (RES) in power grid, especially the wind power [1], [2], the original power source planning and power grid construction are no longer suitable for future development. New challenges for power grid planning occur by the requirement of adaptability, uncertainty, wind curtailment and so on [3], [4]. Moreover, many factors can affect wind power accommodation, and the reasons for wind curtailment in different regions are also different. Generally, system regulation capability, transmission capacity and dispatching mode are the leading factors affecting wind power consumption [5], [6]. The power system regulation capability and transmission capacity should be synthetically considered in the power grid planning to cope with demand and RES development. For regulation capability, the conventional units are generally limited by the generation schedule, the climbing rate, the minimum start up and shut down time, and other operational restrictions. It is hard to timely reduce the power output of the conventional units in the wind peak or load valley periods to provide sufficient consumption space for the wind power. The rapid response capability and dynamic regulation characteristics of energy storage systems (ESSs) can effectively enhance the system regulation capability and wind power acceptance ability [7], [8]. The ESSs can be used in many fields to improve the safe and stable operation, such as ancillary services, power transmission and distribution, renewable energy integration. On the other hand, the transmission congestion is directly caused by limited transmission capacity and uneven power flow distribution. A large number of heavy-load and light-load lines may appear simultaneously

The associate editor coordinating the review of this manuscript and approving it for publication was Lin Zhang.

in the system because of transmission congestion, and it will significantly reduce the system safety margin and development potential. Therefore, enhancing the transmission capacity by transmission network expansion planning (TNEP) [9] and optimizing the power flow distribution in operation process become feasible solutions to alleviate transmission congestion, which makes it highly significant to study the TNEP and ESS planning (ESSP) to cope with the demand and wind power development.

At present, there are many research results for TNEP or ESSP under wind power integration. The TNEP is mixed integer nonlinear programming which may cause computational issues in large-scale system planning. Meanwhile, mathematical optimization and heuristic algorithms are widely applied to solve the TNEP, including mixed integer linear programming (MILP), Bender's decomposition [10], genetic algorithm (GA) and so on. Reference [11] models the TNEP as a two-stage stochastic optimization problem which uses a modified version of Benders' decomposition. Reference [12] proposes a new efficient Benders cuts method for TNEP in which the operation cost and N-1 security criterion are taken into account. Reference [13] considers the effect of distributed generation evaluated by the accurate assessment of loss in TNEP. In addition, a two-stage optimization methodology for security-constrained AC TNEP is developed in [14], which is solved by a modified artificial bee colony algorithm. A multi-objective TNEP model which concerns the correlation between uncertainties related to loads is formulated in [15]. Reference [16] proposes a TNEP method under multiple generation scenarios to significantly reduce the expansion cost with small infeasibilities.

The above literature basically has not considered the wind power integration planning (WPIP). That the wind farms with determinate installed capacity are connected to certain buses is usually assumed. But in fact, the wind power accommodation level, the TNEP, and the ESSP are highly related to the sizing and site of wind farms. Therefore, several researchers try to coordinate the WPIP with the TNEP. The bi-level optimization model is developed for transmission expansion and wind power integration decisions in [17], [18]. The static voltage stability criterion is formulated as operational constraints to obtain more technically and economically schemes for large-scale wind power integration planning and according regional transmission network planning in [19].

The TNEP is mainly aimed at meeting the transmission requirements during peak-load periods. If wind power and load demand fluctuate markedly, the economy and adaptability of the TNEP will be worse. In that case, it is intractable to improve the system flexibility only by the TNEP. However, ESSs can effectively response the regulation requirements from the wind power or load demand. The ESSs which are centralized or distributed are beneficial to peak-load regulation, enhancing transmission ability, alleviating congestion, reducing system reserve capacity and so on. In consequence, the storage duration required to reduce variable generation curtailment is analyzed [20]. Reference [21] examines the curtailment–storage–penetration nexus in the energy transition. Two criteria including maximum regret of wind curtailment cost and total social cost are discussed in a new multi-objective framework for a wind curtailment issue in [22]. References [23]–[25], and [26] explore siting and sizing optimization method of ESSs.

There are still some limitations if TNEP and ESSP separate. Combining TNEP with ESSP can provide a more effective and feasible solution to promote system transmission capacity and regulation capability. Exploring the roles of TNEP and ESSP in a power system becomes more significant than before. Therefore, reference [27] shows the benefit of the TNEP combining with ESSP is greater than each individually. Besides, reference [28] shows that an ESS located at a congestion point has complement effect to further increase the capability of critical transmission corridors. The relationship between transmission and ESSs is discussed in [29], that is, ESSs and transmission lines are not generally substitutes or complements but depend on the actual situation. Moreover, a new robust min-max-min cost optimization model for joint TNEP and ESSP is presented in [30]. Reference [31], [32] achieve the TNEP and ESSP co-optimization scheme considering both long-term and short-term uncertainty. The approach for TNEP considering ESSs in a market-driven environment is described in [33].

The work of the above literature has promoted the development of TNEP and ESSP under wind power integration. However, there are still some issues that can be further explored and studied. In general, most of the literature has not considered the impact of the operation. Actually, with the integration of wind power and ESSs, the coupling between planning and operation is getting stronger. Wind power dispatching, energy storage operation strategy, unit commitment, and other issues should be considered in the planning stage. The planning guided by reasonable operating modes can be eventually more economical, flexible, and practical. In addition, the above literature does not yet involve the power flow distribution optimization during the planning. The transmission redundancy, system security margin, and reliability are highly associated with power flow distribution. Therefore, optimizing the power flow distribution at the planning and operation stages can mitigate transmission congestion and improve system safety margin.

Based on the above analysis, in this paper, the WPIP including the installed capacity and location of the wind farms, the TNEP, ESSP about ESSs locating and sizing and the power generation-side operation are coordinated considered in the planning stage. According to the comprehensive consideration of economy, safety and wind curtailment at the planning and operation level, a source-network-storage joint planning model with the minimizing goal including transmission line expansion cost(TLEC), ESSs construction and operation cost(ECOC), units operation cost(UOC), wind curtailment cost(WCC), heavy-load penalty cost(HLPC) is proposed. Finally, the case analysis is carried out in the

Wood&Wollenberg 6-bus system, the IEEE RTS-24 test system, and the modified IEEE 118-bus system to verify the validity and rationality of the model in different scenarios.

The main contributions of this paper include three aspects:

(1) A novel optimization model which coordinated determines WPIP, TNEP, and ESSP is proposed under comprehensive consideration of economy, safety, and wind curtailment to manage transmission congestion and wind curtailment issue.

(2) The heavy-load transmission is taken into account as a part of the object to enhance the safety margin of the planning scheme. The unit commitment and power flow distribution optimization are involved.

(3) In order to save computational time, new linear ESSs planning & operation constraints and heavy-load operation constraints are formulated in the model. Other constraints such as standard disjunctive model, piecewise linear generation cost, and minimum up-down time constraint are also involved. Compared with the BLP, the effectiveness and precision can be guaranteed by the linearization.

The structure of this paper is organized as follows. Section II provides the problem formulation and the linearization methods of the source-network-storage joint planning model based on MILP. Section III provides the results and analysis of the case study carried out in the Wood&Wollenberg 6-bus system, the IEEE RTS-24 test system, and the modified IEEE 118-bus system to verify the validity and rationality of the proposed model in different scenarios. Section IV summarizes conclusions. For convenience, the list of abbreviations and nomenclatures is provided in Table 1.

TABLE 1. List of variables and constants.

Abbreviations	
BLP	Bi-level programming.
COC	Construction operation cost.
ESS	Energy storage system.
ESSs	Energy storage systems.
ECOC	ESSs construction and operation cost.
ESSP	ESSs planning.
GA	Genetic algorithm.
HLPC	Heavy-load penalty cost.
MILP	Mixed integer linear programming.
O&M	Operation and maintenance.
RES	Renewable energy sources.
TLEC	Transmission line expansion cost.
TNEP	Transmission network expansion planning.
UOC	Units operation cost.
WCC	Wind curtailment cost
WPCR	Wind power curtailment rate
WPIP	Wind power integration planning
Nomenclatures	
Indices	
char	Charging.
disc	Discharging.
de	Demand.
ess/s	ESSs.
g	Thermal power units.
line	Transmission line.
wind/w	Wind farms.
i, j	Index of nodes, belong to Υ_{ess} or Υ_{wind}.
J	Index of block, running from 1 to $N_{segment}$.
l	Index of transmission lines, belong to Ω or Ξ.
n	Index of thermal power units, running from 1 to N_g.
q	Index of ESSs or wind farms, running from 1 to N_{ess} or N_{wind}.
t	Index of time, belong to T_u or T_c.
u	Index of scene, running from 1 to N_{scenes}.
Variables	
$B_{char,t,q,i}$	Maximum charging power of ESS q at node i and time t.
$B_{disc,t,q,i}$	Maximum discharging power of ESS q at node i and time t.
$k_{1,l,t}$,$k_{2,l,t}$,$k_{3,l,t}$	Line status flags.
$L_{s,q,i}$	Location flag of ESS q, which is set to 1 if ESS q is connected to node i and 0 otherwise.
$L_{w,q,i}$	Location flag of wind farm q, which is set to 1 if wind farm q is connected to node i and 0 otherwise.
$P_{char,t,q,i}$	Charging power of ESS q at node i and time t.
$P_{disc,t,q,i}$	Discharging power of ESS q at node i and time t.
$P_{g,n,J,t}$	Power produced in block J of unit n at time t.
$P_{g,n,t}$	Power output of unit n at time t.
$P_{line,l,t}$	Transmission power of line l at time t.
$P_{over,l,t}$	Power exceeding the heavy-load limit of line l at time t.
$P_{s,t,q,i}$	Power output of ESS q at node i and time t.
$P_{w,t,q,i}$	Actual generated electrical power from wind farm q at node i and time t.
$P_{s,q,i}^{rated}$	Rated power of ESS q at node i.
$S_{s,q,i}^{rated}$	Rated capacity of ESS q at node i.
$S_{s,t,q,i}$	Energy stored of ESS q at node i and time t.
$T_{g,on,n,t}$	Start-up duration of unit n at time t.
$T_{g,off,n,t}$	Shut-down duration of unit n at time t.
$U_{g,n,t}$	Status flag which is equal to 1 if unit n is online at time t and 0 otherwise.
$U_{w,q,i}$	Capacity multiplication coefficient of wind farm q at node i.
$X_{char,t,q,i}$	Charging flag of ESS q at node i and time t, which is equal to 1 if ESS q is charged.
$X_{disc,t,q,i}$	Discharging flag of ESS q at node i and time t, which is equal to 1 if ESS q is discharged.
x_l	Binary variable which is equal to 1 if line l needs to be expanded and 0 otherwise.
θ_i , θ_j	Phase angles of the first-end node i, j of line l.
Constants	

II. JOINT OPTIMIZATION MILP MODEL

A. OBJECTIVE FUNCTION

A source-network-storage joint planning model is established for transmission congestion and wind curtailment. The objective function includes five parts: C_{TLEC} for TLEC, C_{ECOC} for ECOC, C_{UOC} for UOC, C_{WCC} for WCC, and C_{HLPC} for HLPC, which is written as (1). The TLEC is represented by the equivalent annual value of the construction cost of expansion lines. The construction cost of ESSs is represented by the equivalent annual value, and the operation and maintenance (O&M) cost of ESSs is represented according to the O&M ratio. The UOC is expressed in terms of the total generation cost of all thermal power units. In addition, transmission lines should retain transmission margin to avoid heavy-load operation. When the transmission power reaches the heavy-load limit, the line can be considered in heavy-load state. The HLPC is imposed on the power exceeding the heavy-load limit.

$$minF = \varepsilon_T C_{TLEC} + \varepsilon_E C_{ECOC} + \varepsilon_U C_{UOC} + \varepsilon_W C_{WCC} + \varepsilon_H C_{HLPC} \quad (1)$$

TABLE 1. *(Continued.)* **List of variables and constants.**

A_{Ξ} ,	Correlation matrix of existing lines.
A_{Ω}	Correlation matrix of candidate lines.
a_n, b_n, c_n	Coefficients of quadratic generation cost function of unit n.
B_l	Susceptance of line l.
c_l	Construction cost of line l.
$C_{capacity}$	Energy cost of ESSs.
C_{power}	Power cost of ESSs.
d	Heavy-load limit factor
d_s	Self-discharging rate.
$e_{sTC,max}$	Ratios of lower limits for the periodic energy stored.
$e_{sTC,min}$	Ratios of upper limits for the periodic energy stored.
K	Wind curtailment price.
L	Heavy-load operation penalty coefficient.
M	A sufficiently large number.
n_{ess}	Lifetime of ESSs.
n_{line}	Lifetime of transmission lines.
N_{ess}	Number of ESSs.
N_g	Number of the units.
N_{scenes}	Number of wind power scenes.
$N_{segment}$	Number of segments of the piecewise linear generation cost function.
N_{wind}	Number of wind farms.
$P_{g,max,n}$	Maximum power output of unit n.
$P_{g,min,n}$	Minimum power output of unit n.
$P_{g,n,J+1}$,$P_{g,n,J}$	Segmentation points of block J+1 and block J of unit n.
$P^{max}_{line,l}$	Transmission power limit of line l.
$P^{rated}_{w,q}$	Basic installed capacity of wind farm q.
$P^{max}_{w,t,q}$	Maximum generated electrical power according to the available wind speed of wind farm q at time t.
$P^{max}_{s,q}$	Maximum rated power of ESS q.
Q_u	Probability of scene u.
R_{om}	O&M ratio of ESSs.
$T^{min}_{g,off,n}$	Minimum down time of unit n.
$T^{min}_{g,on,n}$	Minimum up time of unit n.
$U^{max}_{w,q,i}$	Maximum capacity multiplication coefficient of wind farm q at node i.
$v_{t,q}$	Wind speed of wind farm q at time t.
$v_{in,q}$,$v_{out,q}$,$v_{r,q}$	Cut-in, cut-out and rated wind speeds of wind farm q.
$\alpha_{g,n,J}$	Slope of block J.
$\omega_{g,up,n}$	Ramp-up limit of unit n.
$\omega_{g,down,n}$	Ramp-down limit of unit n.
η	Interest rate.
η_c , η_d	Charging efficiency and discharging efficiency.
Δt	Interval time.
ε_T , ε_E , ε_U , ε_W , ε_H	Weights of components in objective function which are TLEC, ECOC, UOC, WCC, and HLPC respectively.
Sets	
Ω	Candidate lines to be expanded.
Ξ	Existing lines set.
Υ_{ess}	Candidate nodes of ESSs.
Υ_{wind}	Candidate nodes of wind farms.
T_u	Time set in scene u.
T_c	Periodic time.
Functions	
C_{ECOC}	ESSs construction and operation cost.
$C_{ess,q}$	Equivalent annual value of construction cost of ESS q.
$C_{g,n}$	Quadratic generation cost function of unit n.
$\tilde{C}_{g,n,t}$	Piecewise linear generation cost function of unit n.
C_{HLPC}	Heavy-load penalty cost.
C_{TLEC}	Transmission line expansion cost.
C_{UOC}	Units operation cost.
C_{WCC}	Wind curtailment cost.

$$C_{TLEC} = \frac{\eta(1+\eta)^{n_{line}}}{(1+\eta)^{n_{line}}-1}\sum_{l\in\Omega} c_l x_l \tag{2}$$

$$C_{ECOC} = (1+R_{om})\sum_{q=1}^{N_{ess}} C_{ess,q} \tag{3}$$

$$C_{ess,q} = \sum_{i\in\Upsilon_{ess}}\left(\frac{\eta(1+\eta)^{n_{ess}}}{(1+\eta)^{n_{ess}}-1}\left(c_{power}P^{rated}_{s,r,q,i}+c_{capacity}S^{rated}_{s,r,q,i}\right)\right) \tag{4}$$

$$C_{UOC} = \sum_{u=1}^{N_{scenes}} Q_u \sum_{t\in T_u}\sum_{n=1}^{N_g}\left(a_n P^2_{g,n,t} + b_n P_{g,n,t} + c_n\right) \tag{5}$$

$$C_{WCC} = \sum_{u=1}^{N_{scenes}} Q_u K \sum_{q=1}^{N_{wind}}\left\{\sum_{i\in\Upsilon_{wind}}\left(\sum_{t\in T_u}\left(U_{w,q,i}P^{max}_{w,t,q} - P_{w,t,q,i}\right)\right)\right\} \tag{6}$$

$$P^{max}_{w,t,q} = \begin{cases} 0 & v_{t,q} < v_{in,q} \text{ or } v_{t,q} > v_{out,q} \\ \dfrac{v^3_{t,q}-v^3_{in,q}}{v^3_{r,q}-v^3_{in,q}}P^{rated}_{w,q} & v_{in,q} \le v_{t,q} \le v_{r,q} \\ P^{rated}_{w,q} & v_{r,q} < v_{t,q} \le v_{out,q} \end{cases} \tag{7}$$

$$C_{HLPC} = \sum_{u=1}^{N_{scenes}} Q_u L \sum_{t\in T_u}\left(\sum_{l\in\Omega} P_{over,l,t} + \sum_{l\in\Xi} P_{over,l,t}\right) \tag{8}$$

where the optimal installed capacity of wind farm q can be expressed by $U_{w,q,i}P^{rated}_{w,q}$. The Heavy-load operation penalty coefficient depends on the current system running state and reliability requirements. For a system with a small safety margin, the penalty coefficient can be appropriately increased. In addition, decision makers can choose different weights of components according to the scale of each component and decision preferences.

B. CONSTRAINTS

1) Power balance constraint of nodes

$$P_{g,t} + P_{w,t} + P_{s,t} + A_{\Xi}P_{\Xi,t} + A_{\Omega}P_{\Omega,t} = P_{de,t} \tag{9}$$

where $P_{g,t}$, $P_{w,t}$, $P_{s,t}$, and $P_{de,t}$ are the power output vectors of thermal power units, wind farms, ESSs and load at time t respectively; $P_{\Xi,t}$ and $P_{\Omega,t}$ are the transmission power vectors of existing lines and candidate lines at time t, respectively. It is noted that the resistance and copper loss of transmission lines are ignored.

The following assumptions are made for DC model [34]: a. The line susceptances B_{ij} are many times larger than the line conductances G_{ij}, and $B_{ij} \cong -1/x_{ij}$.

b. The angular differences $(\theta_i - \theta_j)$ between typical buses of the system are usually so small.

c. All shunt reactances to ground are eliminated.

d. All bus voltages are assumed to remain constant at nominal values of 1.0 per unit.

2) Existing lines DC power flow constraints

$$P_{line,l,t} + B_l\left(\theta_i - \theta_j\right) = 0 \quad \forall l \in \Xi \tag{10}$$

$$\left|P_{line,l,t}\right| \le P_{line,l}^{max} \quad \forall l \in \Xi \tag{11}$$

3) Expansion lines DC power flow constraints

$$P_{line,l,t} + B_l x_l\left(\theta_i - \theta_j\right) = 0 \quad \forall l \in \Omega \tag{12}$$

$$\left|P_{line,l,t}\right| \le x_l P_{line,l}^{max} \quad \forall l \in \Omega \tag{13}$$

4) Wind farms planning & operation constraints

$$0 \le P_{w,t,q,i} \le U_{w,q,i} P_{w,t,q}^{max} \quad \forall i \in \Upsilon_{wind} \tag{14}$$

$$0 \le U_{w,q,i} \le U_{w,q,i}^{max} L_{w,q,i} \quad \forall i \in \Upsilon_{wind} \tag{15}$$

$$\sum L_{w,q,i} = 1 \quad \forall i \in \Upsilon_{wind} \tag{16}$$

Equation (14) is the upper and lower limits of wind power output, and (15) is the upper and lower limits of the capacity multiplication coefficient. Moreover, the maximum capacity multiplication coefficients at different nodes can be estimated by the natural conditions at different nodes. Equation (16) is the wind farm location constraint, that is, wind farm q can only be connected to one candidate node. The optimal installed capacity and location of the wind farms can be achieved by (14)-(16).

5) The power output constraint of thermal power units

$$U_{g,n,t} P_{g,min,n} \le P_{g,n,t} \le U_{g,n,t} P_{g,max,n} \tag{17}$$

6) The minimum up-down time constraints of thermal power units

$$\begin{cases} \left(U_{g,n,t-1} - U_{g,n,t}\right)\left(T_{g,on,n,t} - T_{g,on,n}^{min}\right) \ge 0 \\ \left(U_{g,n,t} - U_{g,n,t-1}\right)\left(T_{g,off,n,t} - T_{g,off,n}^{min}\right) \ge 0 \end{cases} \tag{18}$$

7) The ramping constraints of thermal power units

$$\begin{cases} P_{g,n,t} - P_{g,n,t-1} \le \omega_{g,up,n} \\ P_{g,n,t-1} - P_{g,n,t} \le \omega_{g,down,n} \end{cases} \tag{19}$$

8) ESSs planning & operation constraints

$$\left|P_{s,t,q,i}\right| \le P_{s,q,i}^{rated} \quad \forall i \in \Upsilon_{ess} \tag{20}$$

$$S_{s,t,q,i} = \begin{cases} (1-d_s) S_{s,t-1,q,i} - \eta_c \Delta t P_{s,t,q,i} & P_{s,t,q,i} \le 0 \\ (1-d_s) S_{s,t-1,q,i} - \frac{1}{\eta_d} \Delta t P_{s,t,q,i} & P_{s,t,q,i} \ge 0 \end{cases} \tag{21}$$

$$0 \le S_{s,t,q,i} \le S_{s,q,i}^{rated} \quad \forall i \in \Upsilon_{ess} \tag{22}$$

$$e_{sTC,min} S_{s,q,i}^{rated} \le S_{s,t,q,i} \le e_{sTC,max} S_{s,q,i}^{rated} \quad \forall t \in T_c \ \forall i \in \Upsilon_{ess} \tag{23}$$

Equation (20) is the power upper and lower limits constraint of ESSs. Equation (21) is the energy stored balance constraint. Equation (22) is the upper and lower limits constraint of the energy stored. Equation (23) is the periodic constraint of the energy stored, that is, the energy stored of the ESSs after periodic operation should be in the interval of $\left[e_{sTC,min} S_{s,q,i}^{rated}, e_{sTC,max} S_{s,q,i}^{rated}\right]$.

9) Heavy-load operation constraints of transmission lines

The key to obtaining the HLPC is judging whether the transmission power has reached the heavy-load limit and calculating the power exceeding the heavy-load limit. Moreover, the power exceeding the heavy-load limit can be calculated by (24)-(25).

$$P_{over,l,t} - P_{line,l,t} + dP_{line,l}^{max} = 0 P_{line,l,t} \ge dP_{line,l}^{max} \tag{24}$$

$$P_{over,l,t} + P_{line,l,t} + dP_{line,l}^{max} = 0 P_{line,l,t} \le -dP_{line,l}^{max} \tag{25}$$

where d is used to characterize the heavy-load limit. Meanwhile, d is belong to [0, 1].

C. LINEARIZED CONSTRAINTS

Since there are quadratic functions, nonlinear constraints, and multi-state judgment processes in the above-mentioned model, which are not conducive to the solution of large-scale system planning problems. Therefore, the following methods are further used for linearization.

1) Expansion lines power flow constraints linearization

There is a product of the binary variable x_l and the continuous variable θ in (12), which makes it be a nonlinear constraint. Hence, the standard disjunctive model [35], [36] can be employed to avoid nonlinearity.

$$\left|P_{line,l,t} + B_l\left(\theta_i - \theta_j\right)\right| \le (1 - x_l) M \quad \forall l \in \Omega \tag{26}$$

When x_l is equal to 1, (26) can be expressed as the DC power flow constraint as (10). When x_l is equal to 0, it indicates that line l does not need to be expanded. Meanwhile, the transmission power of line l has been set to 0 by (13), and (26) is naturally established.

2) ESSs planning & operation constraints linearization

The discharging power and charging power of ESS q can be represented by two state variables $P_{disc,t,q,i}$ and $P_{char,t,q,i}$ respectively. At the same time, five auxiliary variables are introduced for locating and sizing, which are $B_{disc,t,q,i}$, $B_{char,t,q,i}$, $X_{disc,t,q,i}$, $X_{char,t,q,i}$, and $L_{s,q,i}$. Particularly, $P_{disc,t,q,i}$, $P_{char,t,q,i}$, $B_{disc,t,q,i}$, and $B_{char,t,q,i}$ are continuous variables, whereas $X_{disc,t,q,i}$, $X_{char,t,q,i}$, and $L_{s,q,i}$ are binary variables. Then, linearization is performed by (27)-(37). Equation (20) can be converted into (27)-(36), and (21) is changed to (37).

$$P_{s,t,q,i} = P_{disc,t,q,i} + P_{char,t,q,i} \quad \forall i \in \Upsilon_{ess} \tag{27}$$

$$0 \le P_{disc,t,q,i} \le B_{disc,t,q,i} \quad \forall i \in \Upsilon_{ess} \tag{28}$$

$$-B_{char,t,q,i} \le P_{char,t,q,i} \le 0 \quad \forall i \in \Upsilon_{ess} \tag{29}$$

$$0 \le B_{disc,t,q,i} \le P_{s,q}^{max} X_{disc,t,q,i} \quad \forall i \in \Upsilon_{ess} \tag{30}$$

$$0 \le P_{char,t,q,i} \le P_{s,q}^{max} X_{char,t,q,i} \quad \forall i \in \Upsilon_{ess} \tag{31}$$

$$X_{disc,t,q,i} + X_{char,t,q,i} = 1 \quad \forall i \in \Upsilon_{ess} \tag{32}$$

$$0 \le B_{disc,t,q,i} \le P_{s,q,i}^{rated} \quad \forall i \in \Upsilon_{ess} \tag{33}$$

$$0 \le B_{char,t,q,i} \le P_{s,q,i}^{rated} \quad \forall i \in \Upsilon_{ess} \tag{34}$$

$$0 \le P_{s,q,i}^{rated} \le P_{s,q}^{max} L_{s,q,i} \quad \forall i \in \Upsilon_{ess} \tag{35}$$

$$\sum L_{s,q,i} = 1 \quad \forall i \in \Upsilon_{ess} \tag{36}$$

$$S_{s,t,q,i} = (1-d_s) S_{s,t-1,q,i} - \eta_c \Delta t P_{char,t,q,i} - \frac{1}{\eta_d} \Delta t P_{disc,t,q,i} \tag{37}$$

The maximum charging power and discharging power should be less than the rated power according to (33)-(34). The ESS cannot be discharged and charged simultaneously according to (32). ESS q can only be connected to one candidate node by (36). The locating and sizing planning of ESSs can be realized based on (33)-(36).

3) Heavy-load operation constraint linearization

The transmission power of line l has two directions which are positive or negative, and there are two states of line l which are heavy-load or non-heavy load. To this end, (24)-(25) should be linearized. According to the division criterion of the heavy-load limit, the transmission power is further divided into three states, that is, the transmission power can be classified in the interval of $[-1, -d]$, $[-d, d]$, $[d, 1]$ of the transmission limits respectively. Moreover, the line states can be distinguished by (38)-(42), and the power exceeding the heavy-load limit can be calculated.

$$\begin{cases} -P_{line,l}^{max} k_{1,l,t} - dP_{line,l}^{max} k_{2,l,t} + dP_{line,l}^{max} k_{3,l,t} \le P_{line,l,t} \\ P_{line,l,t} \le -dP_{line,l}^{max} k_{1,l,t} + dP_{line,l}^{max} k_{2,l,t} + P_{line,l}^{max} k_{3,l,t} \\ \forall l \in \Omega \cup \Xi \end{cases} \tag{38}$$

$$0 \le P_{over,l,t} - P_{line,l,t} + dP_{line,l}^{max} \le MP_{line,l}^{max} \left(k_{1,l,t} + k_{2,l,t}\right) \tag{39}$$

$$0 \le P_{over,l,t} + P_{line,l,t} + dP_{line,l}^{max} \le MP_{line,l}^{max} \left(k_{2,l,t} + k_{3,l,t}\right) \tag{40}$$

$$0 \le P_{over,l,t} \le P_{line,l}^{max} \left(k_{1,l,t} + k_{3,l,t}\right) \quad \forall l \in \Omega \cup \Xi \tag{41}$$

$$k_{1,l,t} + k_{2,l,t} + k_{3,l,t} = 1 \forall l \in \Omega \cup \Xi \tag{42}$$

Equation (42) indicated that line l can only be in one state at the same time. The function of (38) is to define the state of line l and to generate corresponding line status flags.

(1) When the transmission power of line l is in the interval of $[-dP_{line,l}^{max}, dP_{line,l}^{max}]$, which means line l is non-heavy load, $k_{2,l,t} = 1$ and $k_{1,l,t} = k_{3,l,t} = 0$ are obtained. Meanwhile, $P_{over,l,t}$ should be zero by (41), and (39)-(40) naturally hold.

(2) When the transmission power is in the interval of $[dP_{line,l}^{max}, P_{line,l}^{max}]$, $k_{3,l,t} = 1$ and $k_{1,l,t} = k_{2,l,t} = 0$ are obtained. Then (39) can be converted into (36). The $P_{over,l,t}$ can be calculated by (36), and (40)-(41) are naturally established.

(3) Similarly, if the transmission power is in the interval $[-P_{line,l}^{max}, -dP_{line,l}^{max}]$, $k_{1,l,t} = 1$ and $k_{2,l,t} = k_{3,l,t} = 0$ are obtained. Then (40) is converted into (37), and (39)-(41) are established.

4) Piecewise linear generation cost

Since the generation cost is typically expressed as a quadratic function of the power output, the piecewise linearization method [37] can be used to accurately approximate the quadratic generation cost function, which can be expressed by (44)-(48).

$$C_{g,n} = a_n P_{g,n}^2 + b_n P_{g,n} + c_n \tag{43}$$

$$\tilde{C}_{g,n,t} = C_{g,min,n} U_{g,n,t} + \sum_{J=1}^{N_{segment}} \alpha_{g,n,J} P_{g,n,J,t} \tag{44}$$

$$P_{g,n,t} = \sum_{J=1}^{N_{segment}} P_{g,n,J,t} + U_{g,n,t} P_{g,min,n} \tag{45}$$

$$\alpha_{g,n,J} = \frac{C_{g,n}\left(P_{g,n,J+1}\right) - C_{g,n}\left(P_{g,n,J}\right)}{P_{g,n,J+1} - P_{g,n,J}} \tag{46}$$

$$0 \le P_{g,n,J,t} \le \left(P_{g,n,J+1} - P_{g,n,J}\right) U_{g,n,t} \tag{47}$$

$$C_{g,min,n} = a_n P_{g,min,n}^2 + b_n P_{g,min,n} + c_n \tag{48}$$

5) The minimum up-down time constraint linearization

Equation (18) can be converted into (49) after linearized.

$$\begin{cases} \sum_{m=0}^{T_{g,on,n}^{min}-1} U_{g,n,t+m} \ge T_{g,on,n}^{min} \left(U_{g,n,t} - U_{g,n,t-1}\right) \\ \sum_{m=0}^{T_{g,off,n}^{min}-1} \left(1 - U_{g,n,t+m}\right) \ge T_{g,off,n}^{min} \left(U_{g,n,t-1} - U_{g,n,t}\right) \end{cases} \tag{49}$$

D. SOLUTION ALGORITHM

The source-network-storage joint optimization model belongs to a MILP model, in which the objective function consists of (1)-(8), and the constraints are composed of (9)-(49). The decision variables include binary variables and continuous variables. The binary variables are x_l, $L_{w,q,i}$, $U_{g,n,t}$, $X_{disc,t,q,i}$, $X_{char,t,q,i}$, $L_{s,q,i}$, $k_{1,l,t}$, $k_{2,l,t}$, and $k_{3,l,t}$. The continuous variables are $P_{g,n,t}$, $P_{g,n,J,t}$, $P_{w,t,q,i}$, $U_{w,q,i}$, $S_{s,t,q,i}$, $P_{s,t,q,i}$, $P_{s,q,i}^{rated}$, $S_{s,q,i}^{rated}$, $P_{disc,t,q,i}$, $P_{char,t,q,i}$, $B_{disc,t,q,i}$, $B_{char,t,q,i}$, $P_{line,l,t}$, $P_{over,l,t}$, and θ. Solving the source-network-storage joint optimization model can determine the WPIP scheme, the ESSP scheme, and the TNEP scheme. Particularly, the wind farm integration location can be determined through $L_{w,q,i}$, and $U_{w,q,i} P_{w,q}^{rated}$ can determine the optimal installed capacity of the wind farm at the same time. The integration location of the ESSs can be determined by $L_{s,q,i}$. Moreover, $P_{s,q,i}^{rated}$ and $S_{s,q,i}^{rated}$ are the rated power and capacity of the ESSs respectively. The line expansion plan is achieved by the non-zero value of the x_l. In this paper, the GUROBI solver is called by YALMIP toolbox on MATLAB to solve the proposed source-network-storage joint optimization model. The simulations are carried out with i5-2.6 GHz CPU and 8 GB RAM memory.

III. CASE STUDY

The Wood&Wollenberg 6-bus system [38], the IEEE RTS-24 test system, and the modified IEEE 118-bus system are used to verify the validity and adaptability of the proposed model.

The thermal power units data is shown in Table 9-10 of Appendix. Battery ESSs are used as the example. The parameters of ESSs and transmission lines are shown in Table 11-12. The maximum load of each node is shown in Table 13-14. The transmission lines data of each system is shown in Table 15-16. The rated power of ESSs varies from 0 to 300 MW, and the initial energy stored is 50% of the rated capacity. The charging efficiency and the discharging efficiency are both 0.9. The $e_{sTC,min}$ and $e_{sTC,max}$ are 0.4 and 0.6, respectively. The basic installed capacity of the wind farms is 200MW, the cut-in wind speed is 3 m/s, the cut-out wind speed is 26 m/s, the rated wind speed is 14 m/s. The wind curtailment price and the heavy-load operation penalty coefficient are both 0.0722 $/kWh, and the heavy-load limit factor is 0.8. The number of segments of the piecewise linear generation cost function is 5. The important levels of five components in objective function are considered as sameness so that the weights of the components are set to 1. In order to explore the influence of wind power fluctuation characteristics and anti-peak characteristics, the typical wind power scenes are reconstructed by the "equal-kwh following load" method [39]. The amount of electric quantity generated by the reconstruction wind power scene is the same as the corresponding typical wind power scene. The fluctuation characteristics of the reconstruction wind power scenes are as same as the load characteristics.

A. COMPARISON OF MILP AND BLP MODELS

The joint planning bi-level programming (BLP) model solved by the GA, which is similar to [40], is used to compare with the proposed MILP model. Furthermore, the parameters of GA is set as follow: Population size is 100; the maximum generations is 300; the migration percent is 0.2; and the crossover percent is 0.8.

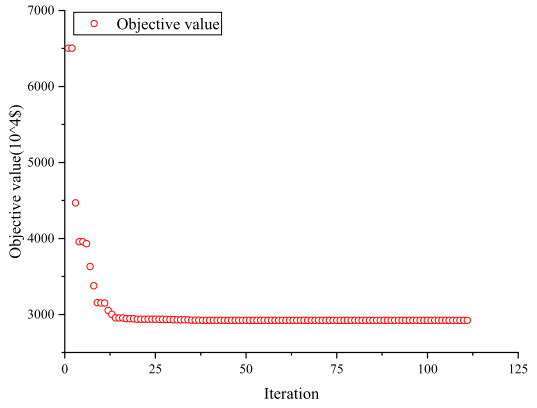

FIGURE 1. The convergence characteristics of the BLP model.

The convergence characteristics of the BLP model is shown in Fig.1. The solution of the MILP model and the BLP model in the Wood&Wollenberg 6-bus system are both shown in Table 2. The optimization results of the MILP model and the BLP model are highly close, which means that, the planning result is credible. Particularly, the largest error comes from the piecewise linear generation cost. Moreover, the solving time of the BLP model is much more than the MILP model. The solving effectiveness of the BLP model is highly depended on the inner layer model solved by GUROBI. In summary, the effectiveness and precision can be guaranteed according to the MILP model, and the MILP model is better than the BLP model.

TABLE 2. The solution of MILP model and BLP model.

Model	MILP	BLP	Error (%)
Line 2(1-4)	1 [a]	1	0.0
Line 3(1-5)	1	1	0.0
Line 5(2-4)	1	1	0.0
Line 7(2-6)	1	1	0.0
Line 9(3-6)	1	1	0.0
Wind farm (MW)	181.0099(5) [b]	181.0099(5)	-3.2e-8
ESS (MW)	31.1455(5)	31.1455(5)	1.3e-8
TLEC (10^4$)	1111.8593	1111.8593	0.0
ECOC (10^4$)	753.7742	753.7742	1.3e-8
UOC (10^4$)	652.6812	652.4391	3.7e-4
WCC (10^4$)	60.4696	60.4697	-5.1e-7
HLPC (10^4$)	345.3305	345.3305	3.5e-8
Total cost (10^4$)	2924.1149	2923.8728	8.3e-5
Time(s)	50137.85	38.04	--

[a] For line $l(ij)$, l is the line number, i and j are the first and end nodes of line l. 0 means that line l does not be expanded, 1 means that the number of expansion lines is one, and 2 means that the number of expansion lines is two.

[b] For convenience of presentation, the installed capacity and location of the wind farm or ESS are represented by 100(1), that is, the installed capacity is 100MW, and the integration node is node 1.

B. THE WOOD & WOLLENBERG 6-BUS SYSTEM

The Wood&Wollenberg 6-bus system has 11 transmission lines and 3 thermal power units. The power generation-side and load-side of the system are relatively independent. Hence, it is conducive to catch obvious effects by changing transmission lines and load. A wind farm and an ESS connected to the grid are considered.

1) Analysis of affecting by HLPC

In order to avoid the transmission line running under heavy-load, the HLPC is introduced to reduce the number of heavy-load lines and heavy-load level at the planning and operation. Two scenarios are set to compare the effect of HLPC as follows: scenario A is the source-network-storage joint planning considering the HLPC, and scenario B is the source-network-storage planning without considering the HLPC. Particularly, the installed capacity of wind farm in scenario B is set as same as scenario A.

The planning scheme under each scenario is shown in Table 3. The construction operation cost (COC) is the sum of TLEC, ECOC, and UOC. Compared to scenario B, line 7 (3-5) is expanded in scenario A. And the HLPC is reduced by about 53.98% in scenario A. The time chart of HLPC is further shown in Fig.2. Obviously, the time of HLPC peak is consistent with the load peak, and the HLPC in scenario A is lower than scenario B at each time. Therefore, it can be believed that considering HLPC can effectively

TABLE 3. The comparison of planning schemes considering HLPC or not.

Scenarios	A	B
Considering HLPC or not	Yes	No
Line 2(1-4)	1	1
Line 3(1-5)	1	1
Line 5(2-4)	1	1
Line 7(2-6)	1	0
Line 9(3-6)	1	1
Wind farm (MW)	181.01(5)	181.01(5)
ESS (MW)	31.15(5)	31.15(5)
TLEC (10^4$)	1111.86	864.78
ECOC (10^4$)	753.77	753.77
UOC (10^4$)	652.68	652.44
WCC (10^4$)	60.47	60.47
HLPC (10^4$)	345.33	750.32
Total cost (10^4$)	2924.11	3081.78
COC (10^4$)	2518.31	2270.99

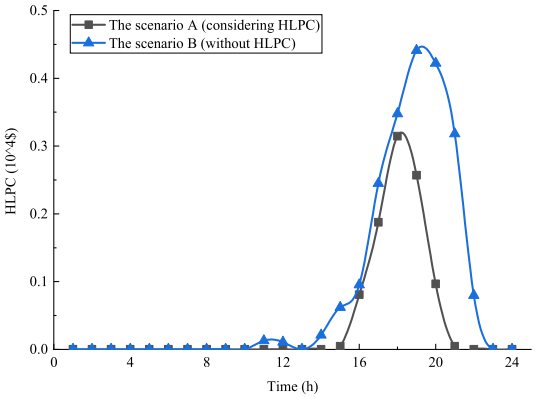

FIGURE 2. The time chart of the HLPC.

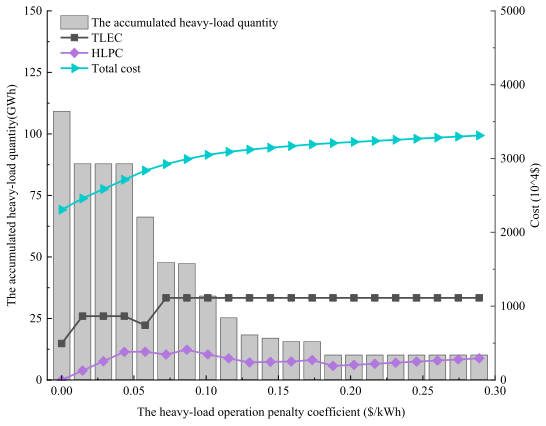

FIGURE 3. The accumulated heavy-load quantity and cost changes.

reduce the heavy-load level, and make the planning scheme and operation schedule more reasonable and reliable.

Furthermore, the heavy-load operation penalty coefficient is increased from 0 to 0.3 to investigate the influence of the penalty coefficient. The accumulated heavy-load quantity and various cost changes are shown in Fig. 3, where the accumulated heavy-load quantity is the sum of the electric quantity exceeding the heavy-load limit of all lines at all times. With the increase of the penalty coefficient, the accumulated heavy-load quantity presents a significant downward trend, and the TLEC and total cost show an overall growth trend. Compared to the penalty coefficient which is 0, the accumulated heavy-load quantity decreases by nearly 56.23% when the penalty coefficient is 0.0722 and decreases by nearly 84.45% when the penalty coefficient is 0.1445. In summary, the value of the heavy-load operation penalty coefficient has a significant influence on the planning result. According to considering the HLPC, the power flow distribution and system safety margin can be effectively optimized during planning and operation, and a more rational planning result and operation schedule can be obtained by balancing economic and safety.

2) Planning schemes in different scenarios

Several scenarios are set up to discuss the role of expansion lines and ESSs, i.e., scenario I is the source-network planning considering TNEP and wind farm locating; scenarios II and III are the source-network-storage planning considering TNEP, ESSP, and wind farm locating; scenario IV is source-network-storage planning considering the TNEP, ESSP, and WPIP which determines the installed capacity and location of the wind farm. Besides, the installed capacity of wind farm in scenarios I and II are 300MW, and it is 500MW in scenario III. The planning content of each scenario are shown in Table 4 and the planning schemes solving in different scenarios are shown in Table 5.

TABLE 4. The planning content of each scenario.

Scenarios		I	II	III	IV
WPIP	Installed capacity	No	No	No	Yes
	Location	Yes	Yes	Yes	Yes
	TNEP	Yes	Yes	Yes	Yes
	ESSP	No	Yes	Yes	Yes

TABLE 5. The planning schemes solving in different scenarios.

Scenarios	I	II	III	IV
Wind farm (MW)	300(5)	300(5)	500(6)	181.01(5)
ESS (MW)	--	57.99(5)	63.82(6)	31.15(5)
Line 2(1-4)	1	1	1	1
Line 3(1-5)	1	0	0	1
Line 5(2-4)	1	1	1	1
Line 7(2-6)	0	0	0	1
Line 8(3-5)	0	0	1	0
Line 9(3-6)	1	1	0	1
Line 11(5-6)	0	0	1	0
TLEC (10^4$)	864.78	494.16	1062.44	1111.86
ECOC (10^4$)	--	1403.42	1544.50	753.77
UOC (10^4$)	599.12	552.25	439.34	652.68
WCC (10^4$)	2316.66	269.27	2691.22	60.470
HLPC (10^4$)	492.66	420.09	453.28	345.33
Total cost (10^4$)	4273.22	3139.21	6190.79	2924.11
COC (10^4$)	1463.90	2449.84	3046.29	2518.31
WPCR	21.30%	2.48%	14.85%	0.92%

First, scenario I and scenario II are compared. The TLEC, UOC, WCC, and HLPC in scenario II are reduced by 42.86%, 7.82%, 88.38%, and 14.73% compared with

TABLE 6. The planning schemes under different wind power scenarios and load factors.

Load factors	1.5	1.5	1	1	0.5	0.5
Wind power scenarios	Typical	Reconstructed	Typical	Reconstructed	Typical	Reconstructed
Wind farm (MW)	816.73(5)	578.79(5)	181.01(5)	362.51(5)	67.02(4)	272.93(6)
ESS (MW)	300.81(4)	35.00(4)	31.15(5)	0.00	0.00	0.00
Line 1(1-2)	0	1	0	0	0	0
Line 2(1-4)	1	1	1	1	0	0
Line 3(1-5)	1	0	1	0	0	0
Line 4(2-3)	1	0	0	0	0	0
Line 5(2-4)	1	1	1	1	0	0
Line 6(2-5)	1	0	0	0	0	0
Line 7(3-5)	1	1	1	0	0	0
Line 8(2-6)	1	0	0	0	0	0
Line 9(3-6)	1	1	1	1	0	0
Line 10(4-5)	1	1	0	0	0	0
Line 11(5-6)	1	1	0	0	0	0
TLEC (10^4$)	2668.46	1853.10	1111.86	494.16	0.00	0.00
ECOC (10^4$)	7280.17	847.06	753.77	0.00	0.00	0.00
UOC (10^4$)	724.76	668.71	652.68	481.56	374.31	155.07
WCC (10^4$)	10554.11	0.00	60.47	0.00	0.00	0.00
HLPC (10^4$)	2938.74	1522.69	345.33	22.12	87.16	43.38
Total cost (10^4$)	24166.25	4891.55	2924.11	997.84	461.47	198.45
COC (10^4$)	10673.40	3368.87	2518.31	975.72	374.31	155.07
WPCR	35.65%	0.00%	0.92%	0.00%	0.00%	0.00%

scenario I, respectively. Meanwhile, line 3(1-5) does not need to expand in scenario II. ESS is helpful to alleviate transmission congestion and enhance transmission capacity. Furthermore, by comparing scenarios II and III with scenario IV, the TLEC and HLPC in scenario III are the largest. It indicates that excessive installed capacity of wind farm may aggravate transmission congestion and construction cost. Besides, the capacity of ESS increases with the increase of wind farm capacity, which indicate that ESS has a greater effect on wind power consumption. Overall, the total cost, WCC, and HLPC in scenario IV are the smallest. The appropriate installed capacity of wind farm is beneficial to avoid the excessive planning of TNEP or ESSP, and it can relatively improve the economics and security margin.

3) Planning schemes under different load factors and wind power scenarios

It is necessary to explore the influence of load growth under existing thermal power level, and the impact of wind power fluctuation characteristics or anti-peak characteristics. Hence, the planning schemes under different load factors and wind power scenarios are shown in Table 6.

In the same wind power scenarios, the COC increases with the increase of the load factor. When the load factor is 0.5, it is not necessary to construct ESSs and expansion lines because the transmission capacity and regulation capability are relatively abundant. When the load factor is 1, the system cannot be operated without wind farms, ESSs or expansion lines because the total demand is greater than total thermal power. After joint planning of WPIP, TNEP, and ESSP, the system can operate under acceptable WCC, HLPC, and wind power curtailment rate (WPCR). When the load factor is 1.5, the installed capacity of wind farm and WPCR of typical scenario are 816.73 MW and 36% respectively. The system demand cannot be guaranteed at demand peak if the installed capacity of wind farm is less. Hence, this installed capacity can be considered as a security capacity to ensure system operation requirement rather than an economic capacity.

Furthermore, when the load factor is 1, the installed capacity of wind farm, the ESS capacity and the various cost of typical scenario are larger than reconstruction scenario. Particularly, the difference between the COC of the typical scenario and reconstructed scenario can be defined as a fluctuating cost for wind power integration. Hence, when the load factors are 1 and 0.5, the fluctuation cost is 15.41 million dollars and 2.19 million dollars respectively.

On the whole, a reasonable source-network-storage planning and operation schedule can improve the load acceptance level under the existing thermal power level. But the excessive load may causes unacceptable COC and WPCR. On the other hand, the transmission congestion and the wind power consumption difficulty will be aggravated because of the fluctuation and anti-peak regulation characteristics of wind power so that more lines and ESSs need to be built for wind power integration.

C. THE IEEE RTS-24 SYSTEM

The IEEE RTS-24 system has 38 transmission lines and 10 thermal power units. It is more favorable to discuss the difference between the centralized and distributed arrangement of ESSs and the impact of generation cost. Hence, four scenarios are set as follows: scenario 1 is the source-network-storage planning under distributed ESSs; scenario 2 and scenario 3 are the source-network-storage planning under centralized ESSs; scenario 4 is the source-network

planning without ESSs integration. The total ESSs capacity in scenario 2 and scenario 3 are set as same as scenario 1. Moreover, the coefficients of the quadratic generation cost function of all units are set as Table 10 in scenarios 1, 3, and 4, while the coefficients of all units are set as unit 1 in scenario 2. The power cost and energy cost of ESSs are set to half of the original.

The planning schemes in different scenarios of IEEE RTS-24 system are shown in Table 7. First, compared to scenario 4, the TLEC in scenario 1 and scenario 3 are reduced by 21.43% and 23.43% respectively. In scenario 1, the HLPC is reduced by 0.31 million dollars while the installed capacity of wind farm is increased by 36.71%. It is shown that ESSs are beneficial to reducing expansion requirement and improving wind power accommodation.

TABLE 7. The planning schemes in different scenarios of IEEE RTS-24 system.

Scenarios	1	2	3	4
ESSs arrangement	distributed	centralized	centralized	--
Coefficient of units	difference	sameness	difference	difference
Wind farm (MW)	1680.25(10)	1851.76(10)	1680.25(10)	1229.00(10)
ESS 1 (MW)	72.451(5)	263.94(10)	263.94(10)	--
ESS 2 (MW)	3.65(18)	--	--	--
ESS 3 (MW)	80.46(11)	--	--	--
ESS 4 (MW)	107.39(10)	--	--	--
Line 3(1-5)	0	0	0	0
Line 4(2-4)	0	1	0	0
Line 7(3-24)	0	0	0	0
Line 9(5-10)	1	1	0	0
Line 10(6-10)	2	2	2	2
Line 11(7-8)	0	2	1	2
Line 13(8-10)	2	0	2	2
Line 15(9-12)	1	0	1	0
Line 17(10-12)	0	0	0	1
Line 18(11-13)	0	0	0	1
Line 23(14-16)	1	1	1	1
Line 26(15-24)	0	0	0	0
Line 27(16-17)	0	1	0	0
Line 33(20-23)	1	0	1	1
TLEC (10^4$)	466.70	356.39	454.82	593.99
ECOC (10^4$)	3193.95	3193.95	3193.95	--
UOC (10^4$)	16725.73	15565.04	16760.75	18936.86
WCC (10^4$)	63.58	0.46	63.58	2107.18
HLPC (10^4$)	0.00	0.00	5.524	31.19
Total cost (10^4$)	20449.96	19115.84	20478.62	21669.22
COC (10^4$)	20386.38	19115.37	20409.51	19530.85
WPCR	0.10%	0.00%	0.10%	4.73%

Furthermore, the impact of generation cost can be obtained according to the comparison between scenario 2 and scenario 3. Particularly, the actual UOC in scenario 2 is 331.22 million dollars if the coefficients of the quadratic generation cost function of all units are set as Table 10. As compared with scenario 2, the TLEC is increased by 27.62%, while the UOC is decreased by 49.40% in scenario 3. Therefore, it can be believed that the thermal power output distribution and power flow distribution is affected by generation cost, that is, the heavy-load level and transmission congestion will be aggravated in local areas because lower cost units tend to generate more power. Hence, it is necessary to consider the generation cost and unit commitment to obtain a more practical planning scheme.

TABLE 8. The planning schemes of modified IEEE 118-bus system.

Scenarios	a	b	c
WPIP	Yes	Yes	Yes
TNEP	Yes	No	Yes
ESSP	No	Yes	Yes
Wind farm (MW)	1163.26(65)	1075.20(65)	2262.28(65)
ESS (MW)	--	36.78(65)	300.00(65)
Line 7(8-9)	1	--	1
Line 8(8-5)	1	--	1
Line 9(9-10)	1	--	1
Line 11(5-11)	1	--	1
Line 51(38-37)	0	--	1
Line 54(30-38)	0	--	1
Line 93(63-59)	1	--	1
Line 94(63-64)	1	--	1
Line 96(38-65)	0	--	1
Line 97(64-65)	1	--	1
Line 99(49-66)	0	--	1
Line 102(65-66)	0	--	1
Line 104(65-68)	1	--	1
Line 119(69-77)	0	--	1
Line 121(77-78)	1	--	1
TLEC (10^4$)	75.05	--	189.76
ECOC (10^4$)	0.00	267.01	2178.15
UOC (10^4$)	24037.41	24808.42	20990.94
WCC (10^4$)	296.92	0.00	107.55
HLPC (10^4$)	0.00	289.14	0.00
Total cost (10^4$)	24409.38	25364.57	23466.41
WPCR	0.70%	0.00%	0.13%

Finally, the difference between the centralized and distributed arrangement of ESSs can be achieved by comparing scenario 1 and scenario 3. In scenario 1, line 9 (5-10) replaces line 11 (7-8), which increases the TLEC by 118.79 thousand dollars. At the same time, the UOC and HLPC decreased by 0.35 million dollars and 55.24 thousand dollars respectively in scenario 1. Relatively, the optimization effect of distributed arrangement is better than centralized arrangement. Distributed ESSs have larger regulating scope and more precise regulating way in the operation process.

D. THE MODIFIED IEEE-118 SYSTEM

The modified IEEE 118-bus system is employed to demonstrate the practicability and effectiveness of the proposed model used in a large power system. The modified IEEE-118 system has 186 existing transmission lines and 54 thermal power units. The detailed parameters of transmission lines and thermal power units are shown in [13], [14]. It is assumed that the demand of each node in modified IEEE-118 system is twice as much as the original. The total thermal power capacity and maximum demand are 9966.20MW and 8484MW respectively. The power cost and energy cost of ESSs are set to 30% of the original. The transmission limit of transmission lines are considered to be 70% of the original. Three scenarios are set with different planning parts. The planning schemes of the modified IEEE 118-bus system are shown in Table 8. The UOC and total cost in scenario b are the maximum while the installed capacity of wind farm are the minimum.

TABLE 9. The thermal power units parameters of Wood & Wollenberg 6-bus system.

Units	Nodes	a_n	b_n	c_n	$P_{g,max,n}$ (MW)	$P_{g,min,n}$ (MW)	Ramping limit (MW/h)	Minimum up-down time (h)
1	1	0.00533	11.669	213.1	200	50	20	6/3
2	2	0.00889	10.333	200	150	37.5	15	3/6
3	3	0.00741	10.833	240	180	45	18	1/3

TABLE 10. The thermal power units data of IEEE RTS-24 test system.

Units	Nodes	a_n	b_n	c_n	$P_{g,max,n}$ (MW)	$P_{g,min,n}$ (MW)	Ramping limit (MW/h)	Minimum up-down time (h)
1	1	0.014142	16.0811	212.3076	480	156	48	3/3
2	2	0.014142	16.0811	212.3076	480	156	48	3/3
3	7	0.052672	43.6615	781.521	750	187.5	75	4/4
4	13	0.00717	48.5804	832.7575	1477.5	517.5	147.75	8/8
5	15	0.00533	11.669	213.1	537.5	165.75	53.75	3/3
6	16	0.00889	10.333	200	387.5	135.75	38.75	2/2
7	18	0.328412	56.564	86.3852	1000	250	100	5/5
8	21	0.008342	12.3883	382.2391	1000	250	100	5/5
9	22	0.008342	12.3883	382.2391	750	150	75	4/4
10	23	0.004895	11.8495	665.1094	1650	621.5	165	12/12

TABLE 11. The parameters of ESSs.

Power cost($/kW)	Energy cost($/kWh)	O&M ratio	During(h)	Interest rate	Lifetime(years)
156.76	465.82	0.02	4	10%	20

TABLE 12. The parameters of transmission lines.

Unit cost ($/km)	Interest rate	Lifetime(years)
144483.62	10%	20

TABLE 13. The maximum load of each node of Wood&Wollenberg 6-bus system.

Nodes	Maximum load (MW)	Nodes	Maximum load (MW)	Nodes	Maximum load (MW)
4	210	5	210	6	210

TABLE 14. The maximum load of each node of IEEE RTS-24 test system.

Nodes	Maximum load (MW)	Nodes	Maximum load (MW)
1	302.40	10	546.00
2	271.60	13	742.00
3	504.00	14	543.20
4	207.20	15	887.60
5	198.80	16	280.00
6	380.80	18	932.40

Contrarily, the UOC and total cost in scenario c are the minimum while the installed capacity of wind farm and TLEC are the maximum. As compared with scenario b, the UOC is decreased by 3.11% in scenario a while it is decreased by 15.39% in scenario c. Expanded transmission lines and ESSs are helpful in wind integration so that the generation cost is significantly reduced. The benefit of the joint planning with WPIP, TNEP, and ESSP is greater than each individually.

TABLE 15. The transmission lines data of Wood&Wollenberg 6-bus system.

Number	First-end node	Transmission limit (MW)	Susceptance (pu)	Length (km)
1	1-2	40	0.2	145
2	1-4	60	0.2	145
3	1-5	40	0.3	218
4	2-3	40	0.25	181
5	2-4	60	0.1	72
6	2-5	30	0.3	218
7	2-6	90	0.2	145
8	3-5	70	0.26	189
9	3-6	80	0.1	72
10	4-5	20	0.4	291
11	5-6	40	0.3	218

TABLE 16. The transmission lines data of IEEE RTS-24 test system.

Number	First-end node	Transmission limit (MW)	Susceptance (pu)	Length (km)
1	1-2	175	0.0139	3
2	1-3	175	0.2112	55
3	1-5	175	0.0845	22
4	2-4	175	0.1267	33
5	2-6	175	0.1920	50
6	3-9	175	0.1190	31
7	3-24	400	0.0839	50
8	4-9	175	0.1037	27
9	5-10	175	0.0883	23
10	6-10	175	0.0605	16
11	7-8	175	0.0614	16
12	8-9	175	0.1651	43
13	8-10	175	0.1651	43
14	9-11	400	0.0839	50
15	9-12	400	0.0839	50
16	10-11	400	0.0839	50
17	10-12	400	0.0839	50
18	11-13	500	0.0476	66
19	11-14	500	0.0418	58
20	12-13	500	0.0476	66
21	12-23	500	0.0966	134
22	13-23	500	0.0865	120
23	14-16	500	0.0389	54
24	15-16	500	0.0173	24
25	15-21	500	0.0490	68
26	15-24	500	0.0519	72
27	16-17	500	0.0259	36
28	16-19	500	0.0231	32
29	17-18	500	0.0144	20
30	17-22	500	0.1053	146
31	18-21	500	0.0259	36
32	19-20	500	0.0396	55
33	20-23	500	0.0216	30
34	21-22	500	0.0678	94

IV. CONCLUSION

A source-network-storage joint planning model which comprehensively considers TLEC, ECOC, UOC, WCC, and HLPC is established for transmission congestion and wind curtailment in this paper. Eventually, the wind power optimal installed capacity and location planning, the transmission network expansion planning, the ESSs locating and sizing planning, and the unit commitment schedule can be obtained by balancing the economy, safety, and wind curtailment.

1) Through the source-network-storage joint planning model, the transmission congestion can be effectively alleviated, and the load acceptance level and wind power accommodation level can be improved under the existing thermal power level. The model is not only suitable for solving

WPIP, ESSP, and TNEP separately, but also suitable for joint planning such as source-network, source-storage, network-storage, and source-network-storage. The model has strong flexibility and applicability as a whole.

2) It can effectively optimize the power flow distribution and heavy-load level during planning and operation by considering the HLPC. Relatively, the system construction and operation cost will increase in order to improve system safety.

3) The wind power fluctuation characteristics and anti-peak characteristics are unfriendly for wind power integration. The fluctuating cost need to be imposed for smoothing fluctuation or balancing power.

4) The ESSs are helpful to alleviate the transmission congestion and reduce the line expansion requirement. The effect of the distributed ESSs is better than the centralized ESSs under the same capacity.

APPENDIX

See Tables 9–16.

REFERENCES

[1] M. S. Nazir, A. J. Mahdi, M. Bilal, H. M. Sohail, N. Ali, and H. M. Iqbal, "Environmental impact and pollution-related challenges of renewable wind energy paradigm—A review," *Sci. Total Environ.*, vol. 683, pp. 436–444, May 2019.

[2] A. Qazi, F. Hussain, N. A. Rahim, G. Hardaker, D. Alghazzawi, K. Shaban, and K. Haruna, "Towards sustainable energy: A systematic review of renewable energy sources, technologies, and public opinions," *IEEE Access*, vol. 7, pp. 63837–63851, 2019.

[3] S. Lumbreras and A. Ramos, "The new challenges to transmission expansion planning. Survey of recent practice and literature review," *Electr. Power Syst. Res.*, vol. 134, pp. 19–29, May 2016.

[4] L. Gacitua, P. Gallegos, R. Henriquez-Auba, A. Lorca, M. Negrete-Pincetic, D. Olivares, A. Valenzuela, and G. Wenzel, "A comprehensive review on expansion planning: Models and tools for energy policy analysis," *Renew. Sustain. Energy Rev.*, vol. 98, pp. 346–360, Dec. 2018.

[5] G.-L. Luo, Y.-L. Li, W.-J. Tang, and X. Wei, "Wind curtailment of China's wind power operation: Evolution, causes and solutions," *Renew. Sustain. Energy Rev.*, vol. 53, pp. 1190–1201, Jan. 2016.

[6] L. Bird, D. Lew, M. Milligan, E. M. Carlini, A. Estanqueiro, D. Flynn, E. Gomez-Lazaro, H. Holttinen, N. Menemenlis, A. Orths, and P. B. Eriksen, "Wind and solar energy curtailment: A review of international experience," *Renew. Sustain. Energy Rev.*, vol. 65, pp. 577–586, Nov. 2016.

[7] G. J. May, A. Davidson, and B. Monahov, "Lead batteries for utility energy storage: A review," *J. Energy Storage*, vol. 15, pp. 145–157, Feb. 2018.

[8] F. Nadeem, S. S. Hussain, P. K. Tiwari, A. K. Goswami, and T. S. Ustun, "Comparative review of energy storage systems, their roles, and impacts on future power systems," *IEEE Access*, vol. 7, pp. 4555–4585, 2018.

[9] R. Hemmati, R.-A. Hooshmand, and A. Khodabakhshian, "State-of-the-art of transmission expansion planning: Comprehensive review," *Renew. Sustain. Energy Rev.*, vol. 23, pp. 312–319, Jul. 2013.

[10] S. Asadamongkol and B. Eua-Arporn, "Transmission expansion planning with AC model based on generalized Benders decomposition," *Int. J. Electr. Power Energy Syst.*, vol. 47, pp. 402–407, May 2013.

[11] S. Lumbreras, A. Ramos, and F. Banez-Chicharro, "Optimal transmission network expansion planning in real-sized power systems with high renewable penetration," *Electr. Power Syst. Res.*, vol. 149, pp. 76–88, Aug. 2017.

[12] O. Alizadeh-Mousavi and M. Zima-Bočkarjova, "Efficient Benders cuts for transmission expansion planning," *Electr. Power Syst. Res.*, vol. 131, pp. 275–284, Feb. 2016.

[13] M. Moradi, H. Abdi, S. Lumbreras, A. Ramos, and S. Karimi, "Transmission expansion planning in the presence of wind farms with a mixed AC and DC power flow model using an imperialist competitive algorithm," *Electr. Power Syst. Res.*, vol. 140, pp. 493–506, Nov. 2016.

[14] S. Das, A. Verma, and P. R. Bijwe, "Security constrained AC transmission network expansion planning," *Electr. Power Syst. Res.*, vol. 172, pp. 277–289, Jul. 2019.

[15] S. Abbasi, H. Abdi, S. Bruno, and M. La Scala, "Transmission network expansion planning considering load correlation using unscented transformation," *Int. J. Electr. Power Energy Syst.*, vol. 103, pp. 12–20, Dec. 2018.

[16] P. F. S. Freitas, L. H. Macedo, and R. Romero, "A strategy for transmission network expansion planning considering multiple generation scenarios," *Electr. Power Syst. Res.*, vol. 172, pp. 22–31, Jul. 2019.

[17] S. Zolfaghari and T. Akbari, "Bilevel transmission expansion planning using second-order cone programming considering wind investment," *Energy*, vol. 154, pp. 455–465, Jul. 2018.

[18] M. Jadidoleslam, A. Ebrahimi, and M. A. Latify, "Probabilistic transmission expansion planning to maximize the integration of wind power," *Renew. Energy*, vol. 114, pp. 866–878, Dec. 2017.

[19] L. Gan, G. Li, and M. Zhou, "Coordinated planning of large-scale wind farm integration system and regional transmission network considering static voltage stability constraints," *Electr. Power Syst. Res.*, vol. 136, pp. 298–308, Jul. 2016.

[20] P. Denholm and T. Mai, "Timescales of energy storage needed for reducing renewable energy curtailment," *Renew. Energy*, vol. 130, pp. 388–399, Jan. 2019.

[21] A. A. Solomon, D. Bogdanov, and C. Breyer, "Curtailment-storage-penetration nexus in the energy transition," *Appl. Energy*, vol. 235, pp. 1351–1368, Feb. 2019.

[22] H. Saber, M. Moeini-Aghtaie, M. Ehsan, and M. Fotuhi-Firuzabad, "A scenario-based planning framework for energy storage systems with the main goal of mitigating wind curtailment issue," *Int. J. Electr. Power Energy Syst.*, vol. 104, pp. 414–422, Jan. 2019.

[23] M. Motalleb, E. Reihani, and R. Ghorbani, "Optimal placement and sizing of the storage supporting transmission and distribution networks," *Renew. Energy*, vol. 94, pp. 651–659, Aug. 2016.

[24] S. Wogrin and D. F. Gayme, "Optimizing storage siting, sizing, and technology portfolios in transmission-constrained networks," *IEEE Trans. Power Syst.*, vol. 30, no. 6, pp. 3304–3313, Nov. 2015.

[25] R. A. Jabr, I. Džafić, and B. C. Pal, "Robust optimization of storage investment on transmission networks," *IEEE Trans. Power Syst.*, vol. 30, no. 1, pp. 531–539, Jan. 2015.

[26] D. Chen, Z. Jing, and H. Tan, "Optimal siting and sizing of used battery energy storage based on accelerating benders decomposition," *IEEE Access*, vol. 7, pp. 42993–43003, 2019.

[27] J. Jorgenson, P. Denholm, and T. Mai, "Analyzing storage for wind integration in a transmission-constrained power system," *Appl. Energy*, vol. 228, pp. 122–129, Oct. 2018.

[28] A. D. Del Rosso and S. W. Eckroad, "Energy storage for relief of transmission congestion," *IEEE Trans. Smart Grid*, vol. 5, no. 2, pp. 1138–1146, Mar. 2013.

[29] P. Neetzow, A. Pechan, and K. Eisenack, "Electricity storage and transmission: Complements or substitutes?" *Energy Econ.*, vol. 76, pp. 367–377, Oct. 2018.

[30] S. Dehghan and N. Amjady, "Robust transmission and energy storage expansion planning in wind farm-integrated power systems considering transmission switching," *IEEE Trans. Sustain. Energy*, vol. 7, no. 2, pp. 765–774, Apr. 2016.

[31] X. Zhang and A. J. Conejo, "Coordinated investment in transmission and storage systems representing long- and short-term uncertainty," *IEEE Trans. Power Syst.*, vol. 33, no. 6, pp. 7143–7151, Nov. 2018.

[32] A. J. Conejo, Y. Cheng, N. Zhang, and C. Kang, "Long-term coordination of transmission and storage to integrate wind power," *CSEE J. Power Energy Syst.*, vol. 3, no. 1, pp. 36–43, 2017.

[33] J. A. Aguado, S. de la Torre, and A. Triviño, "Battery energy storage systems in transmission network expansion planning," *Electr. Power Syst. Res.*, vol. 145, pp. 63–72, Apr. 2017.

[34] J. J. Grainger and W. D. Stevenson, *Power System Analysis*. New York, NY, USA: McGraw-Hill, 2003.

[35] R. V. Villasana, *Transmission Network Planning Using Linear and Linear Mixed Integer Programming*. New York, NY, USA: Rensselaer Polytechnic Institute, 1985.

[36] M. Pereira and S. Granville, "Analysis of the linearized power flow model in benders decomposition," Stanford Univ., Stanford, CA, USA: Tech. Rep. SOL 85-04, 1985.

[37] M. Carrión and J. M. Arroyo, "A computationally efficient mixed-integer linear formulation for the thermal unit commitment problem," *IEEE Trans. Power Syst.*, vol. 21, no. 3, pp. 1371–1378, Aug. 2006.

[38] A. J. Wood and B. Wollenberg, "Power generation operation and control—2nd edition," *Fuel Energy Abstr.*, vol. 3, no. 37, p. 195, 1996.
[39] L. Li *et al.*, "Calculation of wind power variation costs and its application research," *Proc. CSEE*, vol. 36, no. 19, pp. 5155–5163, 2016.
[40] N. Gupta, M. Khosravy, N. Patel, and T. Senjyu, "A bi-level evolutionary optimization for coordinated transmission expansion planning," *IEEE Access*, vol. 6, pp. 48455–48477, 2018.

XIAOSHENG WU received the B.Eng. degree in electrical engineering from the Xiamen University of Technology, China, in 2017. He is currently pursuing the master's degree with Fuzhou University. His research interests include renewable energy integration and optimization operation of power systems.

YUEWEN JIANG received the Ph.D. degree from the College of Electrical Engineering and Automation, Fuzhou University, China, in 2009. In 2016, she was a Guest Researcher with the Department of Electrical Engineering, Technical University of Denmark for one year. She is currently a Professor with Fuzhou University. Her current research interests include electricity market, renewable energy, and optimization operation of power systems.